Temperature stability of a dichroic atomic vapor laser lock

Jessica M. Reeves, Ofir Garcia, and Charles A. Sackett

We have investigated the temperature stability of the dichroic atomic vapor laser lock laser frequency lock method. We find that, in general, the lock exhibits significant temperature sensitivity, leading to laser frequency drifts as large as tens of MHz/K. However, for certain configurations of the optical elements of the system, this temperature dependence is reduced to below 1 MHz/K. These temperature-independent points can be found across a broad range of frequencies. We present a numerical model that reproduces the general behavior of the system. © 2006 Optical Society of America

OCIS codes: 140.2020, 300.6370, 020.7590.

The dichroic atomic vapor laser lock (DAVLL) has been demonstrated in He,[1] Rb,[2] Cs,[3–5] and K (Ref. 6) as an alternative to standard techniques for laser frequency stabilization based on saturated absorption.[7] Compared to standard methods, the DAVLL requires few optical components, making it relatively simple and inexpensive. Other virtues include a large capture range and a widely tunable lock point. These features make the DAVLL especially promising for applications in industrial and field environments. A variety of other simplified saturated absorption techniques have also been proposed,[8–12] but none of these match the DAVLL's capture range and tunability.

For the DAVLL to realize its promise, however, it must reliably hold the laser to one frequency. Both Corwin *et al.*[2] and Beverini *et al.*[4] have observed good stability, with better than 500 kHz peak-to-peak variation over many hours. In contrast, our initial attempts to implement a DAVLL exhibited much larger fluctuations. Certainly many factors may contribute to lock instability. These include temperature drift, magnetic field drift, etaloning and birefringence in the optical components, laser intensity noise, laser alignment fluctuations, and electronic offsets. Our investigations led us to conclude that ambient temperature fluctuations were a dominant contributor to instability in our system. In this paper we discuss the temperature-dependent characteristics of the DAVLL, and show how we have significantly reduced temperature effects on the lock frequency.

The DAVLL method was clearly described by Corwin *et al.*[2] It consists of a vapor cell placed in a longitudinal magnetic field, followed by a quarter-wave retarder and a polarizing beam splitter. The light entering the cell is linearly polarized and can be considered as a superposition of σ^+ and σ^- light. In the magnetic field, the absorption profiles of the σ^+ and the σ^- light are shifted to higher and lower frequencies, respectively. The retarder and polarizing beam splitter separate the circular components, which are measured with two photodiodes. The difference between the two signals is a dispersionlike curve as a function of frequency, which provides an error signal for the lock. The width of the signal is of the order of the Doppler width, $\Delta\nu_d$. Our implementation used a DAVLL with Rb atoms, locked to the ^{87}Rb $S_{1/2}\,F = 2 \leftrightarrow P_{3/2}\,F' = 3$ transition. We note that a variation on the DAVLL, which is optimized for large detunings, is described by Yashchuk *et al.*[13] We have not studied this method extensively, but we have implemented it and observed frequency drifts similar to those discussed here.

As in any servo system, the laser is held at a frequency where the error signal is zero. This frequency (the lock point) can be adjusted by introducing an offset to the dispersion signal. In this way, the entire $\Delta\nu_d$ range is available for locking. The offset can be adjusted in several ways, including rotating the quarter-wave plate, introducing an optical attenuator in one of the beams, or applying an

The authors are with the Department of Physics, University of Virginia, Charlottesville, Virginia 22904. C. A. Sackett's e-mail address is sackett@virginia.edu.

Received 5 May 2005; revised 2 August 2005; accepted 3 August 2005.

0003-6935/06/020372-05$15.00/0

electronic offset to the error signal. We use an optical attenuator consisting of a rotatable polarizer. The polarizer is difficult to adjust with sufficient precision, so we also attenuate the beam with a tilted glass window. By making small adjustments to the tilt angle, very fine control can be achieved.

We found, as noted by Corwin *et al.*,[2] that the first step in achieving good stability with the DAVLL is to use good polarizers. We used calcite polarizers in all cases. In contrast, using dichroic polarizing film or dielectric polarizing beam-splitter cubes caused frequency drifts as large as tens of MHz per hour. For the retarder, we used both a Fresnel rhomb and a zero-order quarter-wave plate with success.

Even with good polarizing optics, we still initially saw day-to-day variations in the lock point of up to 10 MHz, which is inadequate stability for high-precision experiments. Such fluctuations also limit applications of the DAVLL, since the small adjustments needed to correct for this drift would not be possible in a field-deployed device. In an effort to eliminate the fluctuations, we put extra care into the alignment of the optics. We precisely aligned the axis of the polarizer to the axis of the polarizing beam splitter and set the quarter-wave plate axis to $\pm 45°$ as accurately as possible. We then used the optical attenuator to eliminate the residual offset in the error signal, so that far from resonance the signal was zero. Under these conditions, day-to-day repeatability of about 1 MHz was achieved.

Unfortunately, with this alignment, the lock point of the system was about 100 MHz red of the desired transition to the $F' = 3$ excited state. When we reintroduced an offset to tune the lock point back, the stability again deteriorated. We eventually attributed this effect to a variable sensitivity to temperature fluctuations. An important source of temperature sensitivity is the density of the atomic gas, as first noted by Beverini.[4] At room temperature, the density of Rb gas varies by approximately 10% per K.

Changes in density will affect the lock frequency only if the zero crossing of the DAVLL signal is shifted, which happens if the absorption of the σ^+ and σ^- polarizations change by different amounts. Naively, this does not occur when locked to the center of the Doppler profile, because in this case the two polarizations are absorbed symmetrically. However, when the lock point has been displaced with an offset of some kind, the symmetry is lost and temperature dependence is introduced. For instance, if the σ^- beam is attenuated, then the lock point will shift to a higher frequency where the net transmissions for σ^+ and $\sigma^-$are again the same. If the temperature subsequently rises, the atomic absorption of both components will rise by the same fractional amount but the external attenuation will remain constant. Accordingly, the difference between the net transmissions will change, and the lock point will vary. Similar effects occur if the quarter-wave plate is not set at $\pm 45°$.

In reality, understanding the temperature dependence is more complex, because the hyperfine splitting of the excited state is comparable to the Doppler width and the Zeeman width, and this gives an intrinsic asymmetry to the DAVLL signal. To investigate the system in more detail, we developed a computer simulation. We followed the approach described, for instance, by Clifford *et al.*[3] or Beverini *et al.*[4] We model the transmission of laser light through the rubidium cell by calculating the complex transmission amplitudes for each available σ^+ and σ^- transition, assuming the transitions to have Doppler-broadened profiles. The atomic eigenstates and coupling coefficients are calculated by diagonalizing the system Hamiltonian for the $5S_{1/2}$ and $5P_{3/2}$ manifolds, including hyperfine and Zeeman effects. Both the ^{87}Rb and ^{85}Rb isotopes are included since their transitions overlap somewhat. The DAVLL signal is then calculated in terms of the angle θ of the transmission axis of the initial polarizer and the angle ϕ of the fast axis of the quarter-wave plate. Both angles are measured counterclockwise from horizontal, as observed from the output side of the optic. Our magnetic field is directed opposite to the propagation vector of the light.

We used Jones representations for the optics in the system. The light transmitted through the input polarizer has a polarization

$$V_{\text{in}} = \begin{bmatrix} \cos\theta \\ \sin\theta \end{bmatrix}. \tag{1}$$

The transmission of light through the vapor cell is represented as

$$M_{\text{cell}} = \begin{bmatrix} 1 & 1 \\ i & -i \end{bmatrix} \begin{bmatrix} t_+ & 0 \\ 0 & t_- \end{bmatrix} \begin{bmatrix} 1 & -i \\ 1 & i \end{bmatrix}, \tag{2}$$

where t_+ and t_- are transmission coefficients for σ^+ and σ^- light, respectively, and are discussed further shortly. The quarter-wave plate matrix is

$$M_{\lambda/4} = \begin{bmatrix} \cos\phi & -\sin\phi \\ \sin\phi & \cos\phi \end{bmatrix} \begin{bmatrix} 1 & 0 \\ 0 & e^{i\alpha} \end{bmatrix} \begin{bmatrix} \cos\phi & \sin\phi \\ -\sin\phi & \cos\phi \end{bmatrix}, \tag{3}$$

where $\alpha \approx 90°$ is the birefringence of the wave plate. The output polarization is determined by

$$V_{\text{out}} = M_{\lambda/4} M_{\text{cell}} V_{\text{in}} \equiv \begin{bmatrix} H \\ V \end{bmatrix} \tag{4}$$

to find the relative strengths of the two polarizations exiting the DAVLL system. Finally, to model our optical attenuation we included a factor ρ resulting in an output signal $S = |V|^2 - \rho|H|^2$.

The transmission coefficients t_+ and t_- are calculated using

$$t = \exp\left(-\frac{A}{2} + i\beta\right), \tag{5}$$

with amplitude $e^{-A/2}$ and phase β. The amplitude and phase are obtained by summing over allowed transitions $j \leftrightarrow k$:

$$A = \sum_{jk} A_{jk}, \tag{6}$$

$$\beta = \sum_{jk} \beta_{jk}. \tag{7}$$

For each transition,

$$A_{jk}(\nu) = \frac{\sqrt{\pi}}{2}\frac{\Gamma}{w}\, a_{jk} \exp\left[-\left(\frac{\nu - \nu_{jk}}{w}\right)^2\right], \tag{8}$$

$$\beta_{jk}(\nu) = -\frac{\sqrt{\pi}}{2}\, a_{jk}\, F\left(\frac{\nu - \nu_{jk}}{w}\right), \tag{9}$$

where $a_{jk} \equiv \sigma_{jk} n_j L$. Here σ_{jk} is the unbroadened resonant scattering cross section for the $j \leftrightarrow k$ transition, n_j is the temperature-dependent density of Rb atoms in state j, L is the length of the cell, Γ is the natural linewidth, $w \equiv (2k_B T/m\lambda^2)^{1/2}$ parameterizes the Doppler-broadened linewidth, T is the temperature, m is the mass, k_B is Boltzmann's constant, λ is the wavelength of the laser, ν is the laser frequency, ν_{jk} is the resonant frequency, and F is Dawson's integral.[14]

The model neglects effects from optical pumping and saturation, and assumes the magnetic field to be uniform. With these assumptions, we calculate a model DAVLL signal and its temperature dependence.

The experimental system used a Toptica DL100 diode laser system and a 50 mm long Rb vapor cell from Technical Glass, Inc. For the polarizing optics, we used a GT5 polarizer, WPQ zero-order wave plate from Thorlabs, and a PR-15 Rochon polarizing beam splitter from OFR. A second Rb cell was used to make a saturated absorption measurement, which provided a frequency reference as the laser was scanned. Figure 1 shows the DAVLL signals obtained in the experiment and predicted by the model, along with the saturated absorption reference curve. The increasing signals at high frequencies are due to the ^{85}Rb resonance. We do not continue the plot further because nonlinearity of the laser frequency scan introduces a growing error in the frequency scale. The nonlinearity was measured using the location of ^{85}Rb saturated absorption peaks, giving a fractional frequency error of roughly 0.05 GHz^{-1} times the frequency detuning from the ^{87}Rb absorption lines.

Although similar, the experimental and model DAVLL traces differ in detail. Similar disagreement has been noted by other investigators.[3,4] One potential source of discrepancy is stray birefringence of the optical elements, in particular, the cell windows. (Birefringence in the glass windows can be induced by mechanical stress.) We checked for this effect by observing the offset signal introduced by the cell to an off-resonant beam. This yielded an estimated window

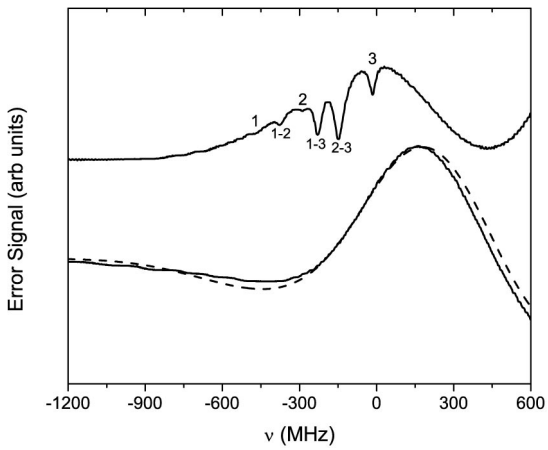

Fig. 1. DAVLL traces. The lower solid curve shows the experimental error signal as a function of frequency for an input polarization angle of $\theta = 90°$ and a wave-plate angle of $\phi = 134°$. The frequency scale is zero at the $F = 2 \leftrightarrow F' = 3$ resonance, as measured using the saturated absorption trace shown by the upper curve. The saturated absorption features are labeled according to excited state, so that 3 marks the $F = 2 \leftrightarrow F' = 3$ transition, and 2–3 marks the crossover between $F = 2 \leftrightarrow F' = 2$ and $F = 2 \leftrightarrow F' = 3$ transitions. The dashed curve is the model prediction. The amplitude of the model is adjusted to match the data, and the wave-plate retardance in the model is set to $\lambda/1.62$ to compensate for the retardance of the cell windows, as discussed in the text. For both the model and the data, the optical attenuation was adjusted to make the signal zero far from resonance.

birefringence of approximately $\lambda/20$. Understanding this birefringence in detail is difficult, since it varies with position on the window and the effects of the first and second windows cannot easily be isolated. We tried to account for it in the model by varying the model values of θ, ϕ, and α. No adjustment of the angles was needed, but the best agreement was obtained when the wave-plate retardance α was raised by approximately $\lambda/17$ to a net value of $\pi/1.62$. This value is used in the all the plots and analyses shown.

Another potential source of error is optical pumping. Our model assumes that all of the ground-state levels are equally occupied, but as the atoms interact with the laser, the level distribution will evolve. The laser beam used had a power of 100 μW and a beam waist of roughly 2 mm, so that an atom would typically scatter approximately ten photons while moving across the beam. Optical pumping effects are thus likely to be important, but incorporating them would require a considerably more sophisticated model. Since we wished to focus on stability effects, we did not pursue this question.

A third potential error is the model assumption that the magnetic field is uniform. Experimentally, the field was generated by placing the cell between two large flexible magnetic sheets with small holes cut in them for the laser beam. The resulting field varied between 105 and 135 G across the length of the cell. Varying the model field across this range had little effect.

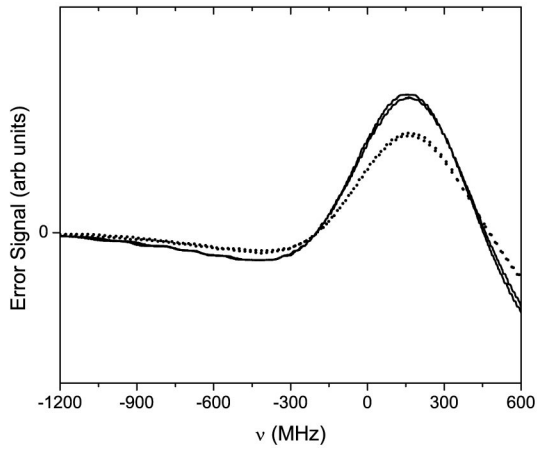

Fig. 2. Temperature sensitivity of DAVLL error signal. The solid traces were measured at a temperature of 26 °C and the dashed traces at 20 °C, for the same polarization settings as in Fig. 1. Two traces are shown at each temperature.

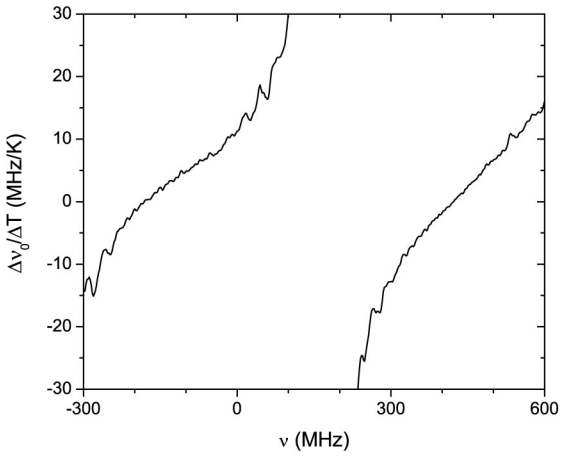

Fig. 3. Temperature sensitivity of DAVLL lock. Using scans such as Fig. 2, the sensitivity of the laser lock frequency ν_0 to temperature T is derived, as described in the text. The temperature sensitivity diverges at the extrema of the error signal curve, here at approximately −400 MHz and +150 MHz. It is not possible anyway to lock the laser near these points because the error signal slope is too small.

The experiment used a DAVLL system that permitted temperature control. The cell had flexible heater strips wrapped around both ends. The heaters sat on a brass mount that was water cooled and held at 20 °C. The temperature of the cell was monitored by using a thermocouple taped to the glass wall. By supplying an ac current of approximately 50 mA to the heaters, the cell could be heated to 26 °C. It took approximately 30 min for the optical signal to equilibrate after changing the temperature.

We measured the lock sensitivity by comparing scans such as those in Fig. 1 at the high and low temperatures. Different scans were aligned using the saturated absorption reference signal. Figure 2 shows typical results obtained, in which a clear variation with temperature is evident. This indicates that the laser lock will also vary with temperature. The sensitivity of the lock point frequency ν_0 can be estimated as

$$\frac{\Delta\nu_0}{\Delta T} \equiv \frac{\Delta S}{\Delta T}\frac{1}{\mathrm{d}S/\mathrm{d}\nu}, \tag{10}$$

where ΔS is the difference between the error signals at the two measured temperatures, ΔT is the temperature difference, and $\mathrm{d}S/\mathrm{d}\nu$ is the average slope of the traces. The result is plotted in Fig. 3 and shows that the temperature sensitivity can be significant.

Fortunately, from Figs. 2 and 3 it is seen that at $\nu = -200$ MHz and $\nu = +400$ MHz the two traces cross and the temperature sensitivity vanishes. We refer to such temperature-independent points as TIPs. Operating the lock near such a TIP is desirable, as it reduces or eliminates the need for temperature stabilization. By varying θ and ϕ, the frequency of the TIP can be set to the desired lock point. Figure 4 shows the measured locations of the TIPs for a range of ϕ. It is seen that a TIP can be placed at basically any frequency where the DAVLL can be locked. In particular, with $\phi = 143°$ we obtained a measured temperature coefficient below 1 MHz/K when locking on the $F = 2 \leftrightarrow F' = 3$ resonance at $\nu = 0$.

Figure 4 also shows the TIP locations predicted by the model. The model reproduces the data fairly well, except in the lower left-hand corner of the graph where the model predicts TIPs that were not observed experimentally. We suspect this is related to the fact that our model trace does not exactly reproduce the experimental trace in that region, as shown in Fig. 1.

The location of the TIPs depends not only on the orientation of the optics, but also on the relative intensities of the two polarizations. Attenuation of one polarization relative to the other changes the shape of

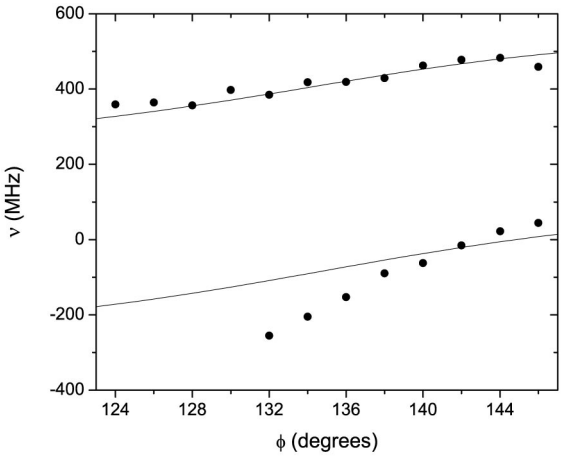

Fig. 4. Location of TIPs. The data points indicate frequencies where the DAVLL is measured to have zero temperature sensitivity, plotted as a function of wave-plate angle ϕ. The input polarizer angle θ was held at 90° and the optical attenuation was adjusted to give zero error signal off resonance. The solid curves show the location of TIPs predicted by the model.

the DAVLL trace and moves the TIPs. So if one identifies a TIP where the error signal is nonzero, then if an attenuator is used to bring the error signal to zero, the TIP location can shift. In our model and data, the attenuation was always chosen to make the error signal zero far from resonance. For instance, in our model we identified a TIP located on resonance at $\phi = 144.8°$. This TIP was not, however, located at the zero crossing of the trace. We needed to change the attenuation factor by about 1% to bring the TIP to zero. In doing so, the TIP shifted by 0.2° to 144.6°. In this particular case, only a small change in attenuation was needed to bring the TIP onto resonance and the shift in TIP location was below the resolution of our experiment. However, this is not true for large attenuation adjustments and the effects of changing relative beam intensities should not be ignored. Using a stable electronic offset will not affect the TIP location, and might therefore be preferable.

In conclusion, the results reported here indicate that temperature fluctuations do indeed have a significant effect on the stability of a DAVLL system. This sensitivity vanishes at certain points, and it is possible to adjust the polarizer, wave plate, and attenuator so that the temperature dependence is small at any desired frequency. Our numerical model supports this understanding, and demonstrates qualitative and quantitative agreement with the experimental results.

We noted previously that Corwin *et al.* achieved good stability without using special angles for their optics, reporting temperature coefficients of 1–2 MHz/K.[2] We believe this is because they were in fact operating near a TIP. The results reported by Corwin *et al.*[2] were for a DAVLL system locked to ^{85}Rb. The excited-state hyperfine splitting of ^{85}Rb is smaller than that of ^{87}Rb, so the asymmetry introduced by the hyperfine effect is reduced. This suggests that the nominal DAVLL set up with $\theta = 0°$ or 90° and $\phi = \pm 45°$ with no additional offset should exhibit a TIP close to the center of the Doppler profile. We confirmed this both experimentally and theoretically. In the experiment, we found a temperature coefficient at the $F = 3 \leftrightarrow F' = 4$ transition below 1 MHz/K for these nominal values. We expect that a similar circumstance also explains the results of Beverini *et al.* for cesium.[4]

We hope that this work has clarified some issues about the stability of DAVLL systems, and that it will allow the DAVLL system to be more widely and successfully applied. We reiterate, however, that the model described here does not exactly reproduce the experimental data, and our predictions are not accurate between −800 and −200 MHz. We expect further progress in this area to help the DAVLL fulfill its potential as a simple, reliable locking method.

This work was supported by the U.S. Office of Naval Research, the National Science Foundation, the Research Corporation, and the Alfred P. Sloan Foundation. We gratefully acknowledge helpful conversations with D. Gauthier and C. Sukenkik.

References

1. B. Cheron, H. Gilles, J. Hamel, O. Moreau, and H. Sorel, "Laser frequency stabilization using Zeeman effect," J. Phys. III **4,** 401–406 (1994).
2. K. L. Corwin, Z.-T. Lu, C. F. Hand, R. J. Epstein, and C. E. Wieman, "Frequency-stabilized diode laser with the Zeeman shift in an atomic vapor," Appl. Opt. **37,** 3295–3298 (1998).
3. M. A. Clifford, G. P. T. Lancaster, R. S. Conroy, and K. Dholakia, "Stabilization of an 852 nm extended cavity diode laser using the Zeeman effect," J. Mod. Opt. **47,** 1933–1940 (2000).
4. N. Beverini, E. Maccioni, P. Marsili, A. Ruffini, and F. Sorrentino, "Frequency stabilization of a diode laser on the Cs D2 resonance line by the Zeeman effect in a vapor cell," Appl. Phys. B **73,** 133–138 (2001).
5. K. R. Overstreet, J. Franklin, and J. P. Shaffer, "Zeeman effect spectroscopically locked Cs diode laser system for atomic physics," Rev. Sci. Instrum. **75,** 4749–4753 (2004).
6. D. J. Gauthier, Duke University, Durham, N.C. 27708 (private communication).
7. W. Demtröder, *Laser Spectroscopy: Basic Concepts and Instrumentation* (Springer, 1996).
8. S. Park, H. Lee, T. Kwon, and H. Cho, "Dispersion-like signals in velocity-selective saturated-absorption spectroscopy," Opt. Commun. **192,** 49–55 (2001).
9. C. Sukenik, H. Busch, and M. Shiddiq, "Modulation-free laser frequency stabilization and detuning," Opt. Commun. **203,** 133–137 (2002).
10. N. Robins, B. Slagmolen, D. Shaddock, J. Close, and M. Gray, "Interferometric, modulation-free laser stabilization," Opt. Lett. **27,** 1905–1907 (2002).
11. G. Wasik, W. Gawlik, J. Zachorowski, and W. Zawadzki, "Laser frequency stabilization by Doppler-free magnetic dichroism," Appl. Phys. B **75,** 613–619 (2002).
12. T. Petelski, M. Fattori, G. Lamporesi, J. Stuhler, and G. Tino, "Doppler-free spectroscopy using magnetically induced dichroism of atomic vapor: a new scheme for laser frequency locking," Eur. Phys. J. D **22,** 279–283 (2003).
13. V. Yashchuk, D. Budker, and J. Davis, "Laser frequency stabilization using linear magneto-optics," Rev. Sci. Instrum. **71,** 341–346 (2000).
14. F. G. Lether, "Constrained near-minimax rational approximations to Dawson's integral," Appl. Math. Comp. **88,** 267–274 (1997).